

The Solar *Hep* Process

Kuniharu Kubodera

Department of Physics and Astronomy, University of South Carolina, Columbia, SC 29208;

e-mail: kubodera@sc.edu

Tae-Sun Park

School of Physics, Korea Institute for Advanced Study, Seoul 130-722, Korea;

e-mail: tspark@kias.re.kr

KEYWORDS: solar burning, solar neutrinos, neutrino oscillations, effective field theory

ABSTRACT: The *Hep* process is the weak-interaction reaction, ${}^3\text{He} + p \rightarrow {}^4\text{He} + e^+ + \nu_e$, occurring in the sun. There is renewed interest in *Hep* owing to current experimental efforts to extract from the observed solar neutrino spectrum information on non-standard physics in the neutrino sector. *Hep* produces highest-energy solar neutrinos although their flux is quite modest, and hence the *Hep* neutrinos can, at some level, influence the solar neutrino spectrum near its upper end. Therefore, a precise interpretation of the observed solar neutrino spectrum requires an accurate estimate of the *Hep* rate. This is an interesting but challenging task. We describe the nature of difficulties involved and how the recent theoretical developments in nuclear physics have enabled us to largely overcome these difficulties. After giving a historical survey of *Hep* calculations, we give an overview of the latest developments, comparing the results obtained in the conventional nuclear physics approach and those obtained in a newly developed effective field theory approach. We also discuss the current status of the experiments relevant to *Hep*.

CONTENTS

INTRODUCTION	3
EARLIER CALCULATIONS	8
RECENT CALCULATIONS – THEORETICAL FRAMEWORK	11
<i>Standard Nuclear Physics Approach (SNPA)</i>	11
<i>Effective Field Theory (EFT)</i>	13
<i>Nuclear EFT in the Weinberg Scheme – Λ-Counting</i>	16
<i>Nuclear EFT in the KSW Scheme – Q-Counting</i>	16
<i>Hybrid EFT</i>	17
<i>EFT* or MEEFT</i>	17
NUMERICAL RESULTS	19
<i>Hep Calculation Based on SNPA</i>	19
<i>Hep Calculation Based on EFT*</i>	19
<i>Off-Shell Problem</i>	20
COMPARISON WITH EXPERIMENTAL DATA	22
RELATED TOPICS	24
<i>The pp Fusion Process</i>	24
<i>Neutrino-deuteron reactions</i>	25
<i>Hen process</i>	25
SUMMARY AND OUTLOOKS	26

1 INTRODUCTION

The *Hep* process, ${}^3\text{He} + p \rightarrow {}^4\text{He} + e^+ + \nu_e$, is one of the thermonuclear reactions occurring in the sun. To explain why this specific process is of current interest, it seems useful to first provide a brief description of the Standard Solar Model, the solar neutrinos and neutrino oscillations.

The sun generates its energy by converting four protons into an alpha particle, $4p \rightarrow {}^4\text{He} + 2e^+ + 2\nu_e$, via series of thermonuclear reactions caused by weak, electromagnetic, or strong interactions. The *pp*-chain, shown in Fig. 1, represents by far the most important scheme by which the $4p \rightarrow {}^4\text{He}$ burning takes place in the sun. To establish how these reactions actually proceed in the sun, one must carry out a detailed simulation in which the radial profiles of the mass density, temperature, chemical composition, etc., are determined in such a manner that hydrostatic equilibrium be satisfied and the empirically known solar properties come out correctly. The principal inputs that go into this simulation are the nuclear reaction rates, equation of state, elemental abundances, and radiative opacity. Over the past four decades a great deal of effort has been invested on this subject, and out of this endeavor has emerged a quantitative model of the sun, called the Standard Solar Model (SSM) (1-5). Among many quantities determined by SSM are the time rates of the thermonuclear reactions occurring in the sun (3); the predicted branching ratios of the various paths involved in the *pp*-chain are given in Fig. 1. Among the reactions featuring in Fig. 1, five are weak-interaction processes that emit solar neutrinos, and SSM predicts the flux ϕ_ν from each source of the solar neutrinos (3); this prediction is shown in Fig. 2. Studying the solar neutrinos is very important for two reasons. First, it gives direct information about the physics of the solar interior, since the neutrinos

exit from the sun practically without experiencing any interactions with the solar medium other than refractive effects (related to the MSW effect to be discussed later). This should be contrasted with the behavior of the photons, which interact with the solar medium so many times that, by the time they reach the surface (after $\sim 40,000$ years !), they do not carry much information about the solar interior. Secondly, the solar neutrinos can provide valuable information on the properties of the neutrinos themselves; the sun is an extremely strong neutrino source and hence can be highly useful for neutrino physics.

The first measurement of the solar neutrinos was done by Davis and his collaborators (6) using a ^{37}Cl target, and the results indicated: [I] The sun indeed emits neutrinos the flux of which is in approximate agreement with the SSM prediction (7), supporting the basic idea of the thermonuclear origin of the solar energy; [II] At a more quantitative level, however, the measured flux is significantly lower than predicted by SSM. This deficit is called the “solar neutrino problem”. The solar neutrino deficit was also confirmed by water Cerenkov counter experiments at the Kamiokande (8) and SuperKamiokande (SK) (9), by gallium-target experiments (10,11), and by heavy-water Cerenkov counter experiments at the SNO (Sudbury Neutrino Observatory) (12). It is to be noted that because of different detection threshold energies (see Fig. 2), these experiments are sensitive to different regions of the solar neutrino spectrum. If we denote by R the ratio of the observed event rate for a given solar neutrino detection experiment to the event rate expected from the SSM prediction, the current status of the solar neutrino problem is summarized as follows: $R = 0.34 \pm 0.03$ for the chlorine experiment (13); $R = 0.465 \pm 0.015$ for the water Cerenkov counter experiment (14); $R = 0.54 \pm 0.03$ for the gallium experiments (15–17); $R = 0.35 \pm 0.02$ (18,19)

and $R = 0.32 \pm 0.02$ (20) for the heavy-water Cerenkov counter experiments. It should be mentioned that the errors attached to the above R 's only include experimental errors. Obviously, the degree of seriousness of the solar neutrino problem ($R < 1$) hinges on the accuracy of the SSM predictions. The latest discussion of the errors to be assigned to the SSM predictions can be found in (3), according to which it is extremely unlikely that the solar neutrino deficit can be attributed to the uncertainties in SSM. This conclusion is further corroborated by highly stringent constraints imposed by the helioseismological data (21).

The above discussion presupposes that the neutrinos created in the sun travel to the terrestrial detectors without changing their identity (or flavor). Let us recall here that there are three distinct neutrinos, ν_e , ν_μ and ν_τ , associated with the electron, muon and tau-lepton, respectively, and that it is ν_e 's that are produced in the sun. If there exists a mechanism (22,23) that changes ν_e into ν_μ and/or ν_τ before it reaches a terrestrial detector that only detects ν_e , then there would be an effective deficit of solar neutrinos. This transmutation of the neutrino flavor, called neutrino oscillations, signals physics that goes beyond the well-established Standard Model of particle physics, and therefore its experimental verification is of paramount importance. Neutrino oscillations can occur either during the neutrino's propagation in vacuum (22,23), or due to the neutrino's interaction with matter (MSW effect) (24).

Now, neutrinos can be detected either via charged-current (CC) reactions or via neutral-current (NC) reactions. Since a CC reaction involves the change $\nu_x \rightarrow x$ ($x = e^-, \mu^-,$ or τ^-), it can occur only for ν_e ; the muon and tau-lepton are too heavy to be created by solar neutrinos. Meanwhile, an NC reaction that involves $\nu_x \rightarrow \nu_x$ occurs with the same amplitude for any neutrino flavor x . At

SNO, the CC reaction $\nu_e d \rightarrow e^- pp$ was used to register the electron neutrino flux ϕ_{ν_e} , while the NC reaction $\nu_x d \rightarrow \nu_x np$ was used to determine the total neutrino flux, $\phi_{\nu,T} \equiv \phi_{\nu_e} + \phi_{\nu_\mu} + \phi_{\nu_\tau}$. The NC reaction data (18) showed that $\phi_{\nu,T}$ agrees very well with the SSM prediction (3), while the CC reaction data (12) indicated $R = 0.347 \pm 0.029$. These results have firmly established flavor transmutations in the solar neutrinos. (For the evidence obtained from comparison of the SNO CC reaction data and the SK data (14), see (12).) Independent evidence for neutrino oscillations is known from the study of the atmospheric neutrinos at SK (25), and from the study of the reactor neutrinos at the KamLAND (26).

Neutrino oscillations occur if a neutrino state produced in a weak-interaction process (“weak eigenstate”) is different from an eigenstate of the Hamiltonian (mass eigenstate), and if the mass eigenstates of different neutrinos are not degenerate. It is conventional to parametrize the former aspect in terms of mixing parameters, and the latter in terms of δm^2 's, differences between the neutrino masses squared. Now that the existence of neutrino oscillations itself has been established, the next important challenge is to determine the accurate values of the mixing parameters and δm^2 's, quantities that should carry valuable information on new physics beyond the Standard Model. (For a recent survey of this topic, see, e.g., (27).) The great importance of this determination makes it highly desirable to assemble an over-constraining body of data, and this is one of the reasons why detailed studies of the solar Hep process can be important.

In discussing Hep , it is convenient to use Bahcall et al.'s latest treatise of SSM (3) as a basic reference (to be called BP00). According to BP00, the neutrino flux due to Hep is $\phi_\nu(hep) = 9.4 \times 10^3 \text{ cm}^{-2}\text{s}^{-1}$, which is seven orders of magnitude smaller than the pp -fusion neutrino flux, and three orders of magnitude smaller

than the ${}^8\text{B}$ neutrino flux $\phi_\nu({}^8\text{B})$; the smallness of $\phi_\nu(\text{hep})$ can also be seen from Fig. 2. [For the radial distribution of sites of *Hep* neutrino generation inside the sun, see Fig. 6.1 in (2).] Because of its extremely small branching ratio (see Fig. 1), *Hep* in fact does not affect solar model calculations. If so, why are we interested in *Hep*? One reason is that *Hep* is a potential source of useful information of non-standard physics in the neutrino sector. *Hep* generates neutrinos of the maximum energy $E_\nu^{\text{max}}(\text{hep}) = 18.8$ MeV, which is higher than that of the ${}^8\text{B}$ neutrinos, $E_\nu^{\text{max}}({}^8\text{B}) = 17$ MeV; thus the *Hep* neutrinos near the upper end of their spectrum represent highest-energy solar neutrinos (see Fig. 2). Solar neutrino detectors like SK and SNO can determine the spectrum of the solar neutrinos in a region dominated by the ${}^8\text{B}$ neutrinos. Meanwhile, the shape of $\phi_\nu({}^8\text{B})$ is independent of solar models to an accuracy of 1 part in 10^5 (28). Therefore, in the absence of *Hep* neutrinos, any deviation of the observed ϕ_ν from $\phi_\nu({}^8\text{B})$ in the higher E_ν region reflects the non-standard behavior of neutrinos. Solar neutrino experiments approaching the level of precision needed for studying this deviation have already been reported from SK (14,29,30) (see below). Apart from the ramifications for neutrino physics, the study of *Hep* neutrinos is also important as a possible additional check of the SSM itself.

In interpreting these and future experiments, we need to know accurately to what extent the *Hep* neutrinos can affect ϕ_ν in the ${}^8\text{B}$ neutrino region (1, 31–33), and for this we must make a reliable estimation of the *Hep* cross section. This task, however, turns out to be a highly non-trivial one. For one thing, although the primary *Hep* amplitude is formally of the Gamow-Teller (GT) type, the usually dominant 1-body GT amplitude is strongly suppressed for *Hep* (see below). Furthermore, the 2-body corrections to the “leading” 1-body GT term

come with opposite sign causing a large cancellation. It is therefore necessary to calculate these “corrections” with great accuracy, which is a highly non-trivial task. Thus, from a nuclear-physics point of view, Hep presents a difficult but at the same time very intriguing challenge.

In what follows, we first present a history of Hep calculations, explaining in more detail the nature of difficulties involved in Hep calculations. We then describe how the recent theoretical developments in nuclear physics have enabled us to largely overcome these difficulties. After reporting the latest results obtained in the so-called standard nuclear physics approach, we shall highlight the results obtained in a newly developed effective field theory approach. We then describe the current status of experimental information on the Hep neutrinos. At the end we discuss several electroweak processes closely related to the Hep calculations.

2 EARLIER CALCULATIONS

An illuminating survey of the earlier Hep calculations can be found in (33,34). The Hep reaction rate can be conveniently expressed in terms of the astrophysical S -factor defined by $S(E) = E\sigma(E)\exp(4\pi\alpha/v_{\text{rel}})$, where $\sigma(E)$ is the Hep cross section at center-of-mass energy E , v_{rel} is the relative velocity between p and ${}^3\text{He}$, and α is the fine structure constant; $S(E)$ is a smooth function of E that remains non-vanishing as $E \rightarrow 0$. The first Hep calculation in 1952 by Salpeter (35) was based on the extreme single-particle picture and only considered the overlap between an s -wave proton scattering wave function and a $1s$ neutron state in ${}^4\text{He}$. This simplified treatment led to a large value for S , $S(0) = 630 \times 10^{-20}$ keV-b, and this value was used by Kuzmin (31), who was the first to discuss Hep in connection with solar neutrinos. Werntz and Brennan

(36) pointed out the drastic suppression of the *Hep* rate due to a specific nature of the initial and final nuclear wave functions. The dominant component of ${}^4\text{He}$ has the orbital configuration, $(1s)^4$, which is totally symmetric, i.e., a state with [4] orbital permutation symmetry. In general, the Pauli principle dictates that a spin-isospin wave function accompanying an orbital function with [4] symmetry must be totally antisymmetric ([1111] state) and hence must have $S=T=0$. The contraposition of this property implies that the p - ${}^3\text{He}$ state with isospin $T=1$ cannot have [4] orbital symmetry. Meanwhile, the 1-body GT operator, $\sum_{i=1}^4 \boldsymbol{\sigma}(i)\tau_-(i)$, acting only on the spin and isospin, cannot change the symmetry properties of orbital wave functions. For *Hep* therefore the leading 1-body GT operator cannot connect the main components of the initial and final states, a feature leading to a drastic suppression of the *Hep* amplitude. This implies that the exchange-current (EXC) effects may play an exceptionally large role here. Werntz and Brennan (36) attempted to relate the *Hep* rate to the M1 matrix element for the *Hen* process, where *Hen* is radiative capture of a thermal neutron on ${}^3\text{He}$: ${}^3\text{He} + n \rightarrow {}^4\text{He} + \gamma$. They assumed: (i) the validity of isospin symmetry apart from the difference in the radial functions of the incident nucleons (proton for *Hep* and neutron for *Hen*); (ii) that 2-body EXC terms dominated for both *Hep* and *Hen* and that their matrix elements could be related to each other via an isospin rotation. Based on the upper limit for the *Hen* cross section known at that time, Werntz and Brennan gave an upper limit for *Hep* S -factor, 3.7×10^{-20} keV-b, which was about 200 times smaller than Salpeter's estimate. Later Werntz and Brennan (37) refined their estimate in several aspects including the addition of the contributions from p -wave capture channels, and they arrived at an S -factor, 8.1×10^{-20} keV-b. Tégen and Bargholtz (38) also attempted to

relate Hep to Hen , but they pointed out the importance of the contributions due to the D -state components in the ${}^3\text{He}$ and ${}^4\text{He}$ wave functions, and they used the EXC operators of the type derived by Chemtob and Rho (39); Tégen and Bargholtz's estimate was $(4 - 25) \times 10^{-20}$ keV-b, where the spread corresponded to the range of the experimental values of the Hen cross section before 1983. This result was sharpened by Wolfs et al. (40), who measured the Hen cross section precisely, reporting a value of $(54 \pm 6) \times 10^{-20}$ μb ; their estimate of the Hep S -factor was $(15.3 \pm 4.7) \times 10^{-20}$ keV-b. Wervelmann et al. (41) also made a precision measurement of the Hen cross section and obtained $(55 \pm 3) \times 10^{-20}$ μb , in good agreement with that obtained by Wolfs et al.; Wervelmann et al., however, predicted for Hep S -factor, $(57 \pm 8) \times 10^{-20}$ keV-b. These estimates should be considered semi-quantitative in nature, since even the estimates of the 1-body terms differ wildly from model to model, and furthermore it is known (39) that the EXC for GT transitions should differ from that for M1 transitions. Subsequently, Carlson et al. (42) showed that there is a significant cancellation between the 1-body and 2-body terms and that the use of realistic wave functions (as opposed to schematic wave functions employed in the previous calculations) is crucial for a reliable estimation of the Hep rate. These authors performed a variational Monte Carlo calculation and, with the use of EXC operators derived from pion-, ρ -exchange diagrams and Δ -excitation diagrams, they obtained $S = 1.3 \times 10^{-20}$ keV-b (42). Schiavilla et al. (43) performed a similar calculation but with the explicit Δ degree of freedom and obtained $S = (1.4 - 3.2) \times 10^{-20}$ keV-b. The Hep calculations up to this point only considered the contribution of the s -wave capture channel, except for the work of Werntz and Brennan (37). Horowitz (44) presented a new estimate of the contribution of the p -wave cap-

ture channel, using schematic wave functions, and emphasized that it could be of substantial magnitude. We shall categorize *Hep* estimations that have appeared since 2000 as “recent” calculations and discuss them in the next section.

As the above survey shows, the calculated value of the *Hep* *S*-factor changed by two orders of magnitude from the original Salpeter value, reflecting a number of subtle aspects involved. Fortunately, however, an encouraging sign of convergence in the *Hep* *S*-factor has been emerging over the past few years. Firstly, this is due to further significant progress along the line of work following (42,43). Secondly, the application of effective field theory to *Hep* has greatly increased the reliability of the calculated *S*-factor. These latest developments are the subjects of the following sections. To present them in a coherent manner, we will first survey the relevant theoretical frameworks in a somewhat general context, and then proceed to discuss the specific numerical results for *Hep*.

3 RECENT CALCULATIONS – THEORETICAL FRAMEWORK

3.1 Standard Nuclear Physics Approach (SNPA)

The phenomenological potential picture has been highly successful in describing a great variety of nuclear phenomena. In this picture a model Hamiltonian for an *A*-nucleon system involves a phenomenological 2-body potential v^{phen} (and, if needed, an additional phenomenological 3-body potential). Once this model Hamiltonian is specified, the nuclear wave function is obtained by solving the *A*-body Schrödinger equation. Recent progress in numerical techniques for this type of calculation has reached such a level (45) that the wave functions of low-lying levels for light nuclei can now be obtained practically with no approximation. This achievement frees us from the “usual” nuclear physics complications that

arise as a result of truncation of nuclear Hilbert space down to certain model space (such as shell-model configurations, cluster-model trial functions, etc.). As there is large freedom in choosing a possible form for the short-range part of v^{phen} , one assumes a certain functional form and fixes the parameters appearing in it by demanding that the nucleon-nucleon (NN) scattering data and the deuteron properties be reproduced. There are by now a number of so-called high-precision phenomenological potentials that can reproduce all the existing 2-nucleon data with normalized χ^2 values close to unity. In normal circumstances, nuclear responses to external electroweak probes are given, to good approximation, by 1-body terms; these are also called the impulse approximation (IA) terms. To obtain higher accuracy, however, one must also consider exchange current (EXC) terms, which represent the contributions of nuclear responses involving two or more nucleons. In particular, if for some reason the IA contributions are suppressed, it becomes essential to take account of the EXC contributions. These EXC's are usually derived from 1-boson exchange diagrams, imposing the low-energy theorems and current algebra properties on the vertices featuring in the diagrams (39, 46, 47). A formalism based on this picture shall be referred to as the standard nuclear physics approach (SNPA). (This is also called a potential model in the literature.) SNPA has been used extensively for describing nuclear electroweak processes in light nuclei, and general good agreement found between theory and experiment (45) gives a strong indication that SNPA captures much of the physics involved. The calculations in (42, 43) quoted earlier represent the early stage of SNPA.

3.2 Effective Field Theory (EFT)

Although SNPA has been scoring undeniable successes in correlating and explaining a vast variety of data, it is still important from a fundamental point of view to raise the following issues. First, since hadronic systems are governed by quantum chromodynamics (QCD), one should ultimately be able to relate nuclear phenomena with QCD, but this relation is not visible in SNPA. In particular, while chiral symmetry is known to be a fundamental symmetry of QCD, SNPA is largely disjoint from this symmetry. Secondly, in SNPA, even for describing low-energy phenomena, we start with a “realistic” phenomenological potential which is tailored to encode short-range (high-momentum) and long-range (low-momentum) physics simultaneously. This mixing of the two different scales seems theoretically dissatisfactory. Thirdly, in writing down a phenomenological Lagrangian for describing the nuclear interaction and nuclear responses to the electroweak currents, SNPA is not equipped with a clear guiding principle; it is not obvious whether there is any identifiable expansion parameter that helps us to control the possible forms of terms in the Lagrangian and that provides a general measure of errors in our calculation. To address these and other related issues, a new approach based on EFT was proposed (48) and it has been studied with great intensity; for reviews, see, (49, 50).

The intuitive picture of EFT is in fact rather simple. In describing phenomena characterized by a typical energy-momentum scale Q , we expect that we need not include in our Lagrangian those degrees of freedom that pertain to energy-momentum scales much higher than Q . This expectation motivates us to introduce a cut-off scale Λ that is sufficiently large compared with Q and classify our fields (to be generically represented by Φ) into two groups: high-frequency

fields Φ_{high} and low-frequency fields Φ_{low} . By eliminating (or *integrating out*) Φ_{high} , we arrive at an *effective* Lagrangian that only involves Φ_{low} as explicit dynamical variables. Using the notion of path integrals, the effective Lagrangian \mathcal{L}_{eff} is related to the original Lagrangian \mathcal{L} as

$$\int [d\Phi] e^{i \int d^4x \mathcal{L}(\Phi)} = \int [d\Phi_{low}] e^{i \int d^4x \mathcal{L}_{eff}(\Phi_{low})}. \quad (1)$$

One can show that \mathcal{L}_{eff} defined by eq.(1) inherits the symmetries (and the patterns of symmetry breaking, if there are any) of \mathcal{L} . It also follows that \mathcal{L}_{eff} should be the sum of all possible monomials of Φ_{low} and their derivatives that are consistent with the symmetry requirements dictated by \mathcal{L} . Since a term involving n derivatives scales like $(Q/\Lambda)^n$, the terms in \mathcal{L}_{eff} can be organized into a perturbative series in which Q/Λ serves as an expansion parameter. The coefficients of terms in this expansion scheme are called the low-energy constants (LECs). Insofar as all the LEC's up to a specified order n can be fixed either from theory or from fitting to the experimental values of the relevant observables, \mathcal{L}_{eff} serves as a complete (and hence model-independent) Lagrangian to the given order of expansion.

In applying EFT to nuclear physics, the underlying Lagrangian is the QCD Lagrangian \mathcal{L}_{QCD} , whereas, for the typical nuclear physics energy-momentum scale $Q \ll \Lambda_\chi \sim 1$ GeV, the effective degrees of freedom that would feature in the effective Lagrangian \mathcal{L}_{eff} are hadrons rather than the quarks and gluons. It is not obvious how to apply the formal definition, eq.(1), for establishing a relation between \mathcal{L}_{QCD} and \mathcal{L}_{eff} written in terms of the hadrons, since the hadrons cannot be simply identified with the low-frequency field, Φ_{low} , in the original Lagrangian. At present, the best one could do is to resort to symmetry considerations and the above-mentioned expansion scheme. Here chiral symmetry plays an important

role. It is known that chiral symmetry is spontaneously broken, generating the pions as Nambu-Goldstone bosons. This feature can be incorporated by assigning suitable chiral transformation properties to the Goldstone bosons and writing down all possible chiral-invariant terms up to a specified chiral order, see, e.g., (51). The above consideration presupposes exact chiral symmetry in \mathcal{L}_{QCD} . In reality, \mathcal{L}_{QCD} contains small but finite quark mass terms, which explicitly violate chiral symmetry and lead to a non-vanishing value of the pion mass m_π . Again, there is a well-defined method to determine what terms are needed in the Goldstone boson sector to represent the effect of explicit chiral symmetry breaking (51). One can then establish a counting rule, called the chiral counting, which allows us to classify the relative importance of a term in \mathcal{L}_{eff} and a given Feynman diagram according to the number of powers in Q/Λ and m_π/Λ . These considerations lead to an EFT called chiral perturbation theory (χPT) (52, 53).

The successes of χPT in the meson sector are well known; see, e.g., (49). A problem we encounter in extending χPT to the nucleon sector is that, as the nucleon mass m_N is comparable to the cut-off scale Λ_χ , a simple application of expansion in Q/Λ does not work. This problem can be circumvented by employing heavy-baryon chiral perturbation theory ($\text{HB}\chi\text{PT}$) (54). $\text{HB}\chi\text{PT}$ has been used with great success to the 1-nucleon sector, see, e.g., (49). $\text{HB}\chi\text{PT}$, however, cannot be applied in a straightforward manner to nuclear systems, because nuclei involve very low-lying excited states, and the existence of this small energy scale spoils the original counting rule (48).

3.3 Nuclear EFT in the Weinberg Scheme – Λ -Counting

Weinberg proposed to avoid this difficulty as follows (48). Classify Feynman diagrams into two groups, irreducible and reducible diagrams. Irreducible diagrams are those in which every intermediate state has at least one meson in flight; all others are classified as reducible diagrams. We then apply the above-mentioned chiral counting rules only to irreducible diagrams. The contribution of all the 2-body irreducible diagrams (up to a specified chiral order) is treated as an effective potential acting on nuclear wave functions. Meanwhile, the contributions of reducible diagrams can be incorporated by solving the Schrödinger equation. This two-step procedure may be referred to as *nuclear* χ PT or, to be more specific, nuclear χ PT in the Weinberg scheme.

To apply nuclear χ PT to a process that involves (an) external current(s), we derive a nuclear transition operator \mathcal{T} by evaluating the complete set of irreducible diagrams (up to a given chiral order ν) involving the relevant external current(s). For consistency in chiral counting, the nuclear matrix element of \mathcal{T} must be calculated with the use of nuclear wave functions which are governed by nuclear interactions that represent all the irreducible A -nucleon diagrams up to ν -th order. If this program is carried out exactly, it would constitute an ab initio calculation. The unambiguous classification of transition operators according to their chiral orders is a great advantage of EFT, which is missing in SNPA.

3.4 Nuclear EFT in the KSW Scheme – Q -Counting

There exists an alternative form of nuclear EFT based on the power divergence subtraction (PDS) scheme. The PDS scheme proposed by Kaplan, Savage and Wise in their seminal papers (55) uses a counting scheme (often called Q -

counting) that is different from the Weinberg scheme. Although a great number of important investigations have been made using the PDS scheme (for a review, see, e.g., (56)), here we shall be primarily concerned with the Weinberg scheme. The reason is that the PDS scheme has so far been used chiefly for the 2-nucleon systems (see, however, (57–59)) and hence its connection with the *Hep* process is at present less direct than the Weinberg scheme is; no *Hep* calculations based on the PDS scheme exist in the literature at the time of this writing.

3.5 Hybrid EFT

In the preceding subsections we emphasized the formal merits of nuclear EFT. In actual calculations, however, it is still a big challenge to generate, strictly within the EFT framework, nuclear wave functions whose accuracy is comparable to that of SNPA wave functions (see section 7, however). A pragmatic solution to this problem is to use wave functions obtained in SNPA; we refer to this eclectic approach as hybrid EFT (60–62). Since the *NN* interactions that generate SNPA wave functions reproduce accurately the 2-nucleon data, the use of hybrid-EFT is almost equivalent to using the empirical data themselves to control the initial and final nuclear wave functions, insofar as the off-shell problem (see below) and the contributions of 3-body (and higher-body) interactions are properly addressed.

3.6 EFT* or MEEFT

Hybrid EFT can be used for light complex nuclei ($A = 3, 4, \dots$) with essentially the same accuracy and ease as for the $A=2$ system. We should emphasize in this connection that, in A -nucleon systems ($A \geq 3$), the contributions of transition operators involving three or more nucleons are intrinsically suppressed according

to chiral counting, and hence, up to a certain chiral order, a transition operator in an A -nucleon system consists of the same EFT-based 1-body and 2-body terms as used for the 2-nucleon system.

As mentioned earlier, the chiral Lagrangian is definite only when the values of all the relevant LECs are fixed, but there may be cases where this condition cannot be readily met. Suppose that a 2-body EXC operator under consideration contains an LEC (call it κ) that cannot be determined with the use of $A=2$ data alone. It is possible that an observable (call it Ω) in a A -body system ($A \geq 3$) is sensitive to κ and that the experimental value of Ω is known with sufficient accuracy. Then we can determine κ by calculating the hybrid-EFT matrix element corresponding to Ω and adjusting κ to reproduce the empirical value of Ω . Once κ is fixed this way, we can make *predictions* for any other observables for any other nuclear systems that are controlled by the same transition operators. Hybrid EFT used in this manner is referred to as EFT*, or as MEEFT (more effective EFT).

The effective Lagrangian \mathcal{L}_{eff} is, by construction, valid only below the specified cutoff scale Λ . This basic constraint should be respected in nuclear EFT calculations as well. One way to implement this constraint is to introduce a momentum-cutoff Λ for the 2-nucleon relative momentum. The sensitivity of the results on the choice of Λ is expected to serve as a measure of uncertainties in the calculational framework.

4 NUMERICAL RESULTS

4.1 *Hep* Calculation Based on SNPA

Marcucci et al. have recently carried out a highly elaborate SNPA calculation of the *Hep* rate (34, 63). The treatment of the 4-body wave functions was improved with the use of the correlated-hyperspherical-harmonics method (64). The strength of the dominant EXC contribution due to a Δ -excitation diagram was adjusted to reproduce the experimental value of $\Gamma_{\beta}^{\text{tritium}}$, the tritium beta-decay rate: $\Gamma_{\beta}^{\text{tritium}}(\text{exp}) = (1.5409 \pm 0.0035) \times 10^{-4} \text{ day}^{-1}$ (65). This type of empirical normalization, first introduced in (42), is expected to reduce significantly the model dependence of the calculated *Hep* rate. Furthermore, the contribution of the initial *p*-wave channel was included. The resulting *Hep* *S*-factor at 10 keV (close to the Gamow peak) is $S = (10.1 \pm 0.6) \times 10^{-20} \text{ keV-b}$; this is the value used in BP00 (3). The corresponding threshold value is $S = 9.64 \times 10^{-20} \text{ keV-b}$.

4.2 *Hep* Calculation Based on EFT*

Park et al. (66, 67) carried out an EFT* calculation of the *Hep* rate, considering up to next-to-next-to-next-to-leading order in chiral counting. To this order, there appears in 2-body terms one LEC that at present cannot be determined from data belonging to the $A=2$ systems. This unknown LEC, denoted by \hat{d}_R in (62), parametrizes the strength of contact-type four-nucleon axial-current coupling. Park et al. noted that \hat{d}_R also features as the only unknown parameter in the calculation of $\Gamma_{\beta}^{\text{tritium}}$, and determined \hat{d}_R from the experimental value of $\Gamma_{\beta}^{\text{tritium}}$ (65). With the value of \hat{d}_R determined this way, Park et al. made a parameter-free EFT* calculation of the *Hep* rate (66, 67). The result for the

threshold S -factor is $S = (8.6 \pm 1.3) \times 10^{-20}$ keV-b, where the error spans the range of the Λ dependence. This EFT* result supports the SNPA results in (34, 63). It is reasonable to expect that, if the effects of neglected higher-order terms and deviations from the framework of EFT* itself are sizable, they would cause the significant Λ dependence in the calculated S . This consideration led the authors of (66, 67) to adopt the Λ dependence ($\sim 15\%$ variation) of S_{Hep} as a measure of uncertainties in their EFT* calculation of S_{Hep} . The afore-mentioned large cancellation between the 1-body and 2-body contributions in Hep amplifies the Λ dependence of S_{Hep} up to $\sim 15\%$, but this dependence is still reasonably small. (Later we shall discuss the pp -fusion reaction, where there is no such cancellation and the Λ dependence is found to be extremely small.) In Fig.2, the 15% errors assigned to $\phi_\nu(hep)$ reflects the uncertainty in the EFT* estimation of S_{Hep} in (66, 67); this is the first time that $\phi_\nu(hep)$ is presented with an error estimate attached.

4.3 Off-Shell Problem

The use of hybrid EFT may bring in a certain degree of model dependence due to the off-shell effects, because the phenomenological NN interactions are constrained only by the on-shell 2-nucleon observables. This off-shell effect, however, is expected to be small for the reactions under consideration, since they involve low momentum transfers and hence are not extremely sensitive to the short-range behavior of the nuclear wave functions. One way to quantify this expectation is to compare a 2-nucleon relative wave function generated by the phenomenological potential with that generated by an EFT-motivated potential. Phillips and Cohen (68) made such a comparison in their analysis of the 1-body operators

responsible for electron-deuteron Compton scattering, and showed that a hybrid EFT should work well up to momentum transfer 700 MeV. A similar conclusion is expected to hold for a 2-body operator, so long as its radial behavior is duly “smeared-out” reflecting a finite momentum cutoff. Thus, EFT* as applied to low energy phenomena is expected to be practically free from the off-shell ambiguities.

Another indication of the stability of the EFT* results comes from a recently developed idea of the “low-momentum nuclear potential”. Let us recall that a “realistic phenomenological” potential v^{phen} is determined by fitting to the 2-nucleon data up to the pion production threshold energy. So, physically, v^{phen} should reside in a momentum regime below a certain cutoff Λ_c . In the conventional treatment, however, the existence of this cutoff scale is ignored. Bogner et al. (69) proposed to construct an *effective low-momentum* potential V_{low-k} by integrating out from v^{phen} the momentum components higher than Λ_c , and calculated V_{low-k} ’s corresponding to a number of well-established NN potentials. Remarkably, the resulting V_{low-k} ’s were found to lead to identical half-off-shell T -matrices for all the cases studied, even though the ways short-range physics is encoded in these v^{phen} ’s are quite diverse. This implies that the V_{low-k} ’s are free from the off-shell ambiguities, and therefore the use of V_{low-k} ’s is essentially equivalent to employing an EFT-based NN potential. Now, the fact EFT* calculations by design contain a momentum-cutoff regulator essentially ensures that an electroweak transition matrix element calculated in EFT* is only sensitive to those half-off-shell T -matrices that are controlled by V_{low-k} , and therefore the EFT* results reported in (67) are expected to be essentially free from the off-shell ambiguities.

Furthermore, since correlating the observables in neighboring nuclei (as was done here) is likely to serve as an additional renormalization, the possible effects of higher chiral order terms and/or off-shell ambiguities can be significantly suppressed by the use of EFT*

5 COMPARISON WITH EXPERIMENTAL DATA

In SK experiments, information on the solar neutrino spectrum ϕ_ν was obtained by detecting the recoil electron in the reaction, $\nu + e^- \rightarrow \nu + e^-$, for $E_{\text{recoil}} \geq 6.5$ MeV in (29), and for $E_{\text{recoil}} \geq 5$ MeV in (14). As mentioned, ϕ_ν in this range is governed by the ^8B neutrinos with a tiny mixture of hep neutrinos. In (29), the data are presented in 15 bins between 6.5 MeV and 14 MeV and one higher-energy bin covering 14 - 20 MeV. The three highest bins showed a larger number of events than expected from the then most popular neutrino oscillation parameters. Bahcall and Krastev (33) made a detailed analysis of these data considering various neutrino oscillation scenarios and treating the Hep S -factor, S_{Hep} , as an adjustable parameter. The philosophy behind this treatment was that, although the “1998 standard value” of S_{Hep} adopted in (70) came from an elaborate SNPA calculation (43), a “first-principle physics argument” was still missing to exclude the possibility that S_{Hep} might exceed, e.g., 10 times this value. Introducing the enhancement factor α defined by $\alpha \equiv S_{Hep}/(2.3 \times 10^{-20} \text{ keV-b})$, where the denominator is the central value of the 1998 standard S_{Hep} , Bahcall and Krastev reported that, by allowing α to be larger than 20, one could improve significantly global fits to all the then available solar neutrino data for every case of the neutrino oscillation scenarios studied. This result triggered renewed theoretical efforts by Marcucci et al. (34, 63) and by Park et al. (66, 67) to determine S_{Hep}

with higher accuracy. An improved SNPA calculation by Marcucci et al. (34,63) gave a value of S_{Hep} 4.4 times larger than the “1998 standard value”; the value of $\phi_\nu(hep)^{SSM}$ appearing in BP00 (3) is based on Marcucci et al.’s S_{Hep} . It is to be noted that the authors of (3) avoided giving an estimate of total uncertainty in $\phi_\nu(hep)^{SSM}$, quoting the unique subtlety involved in the calculation of S_{Hep} .

According to the more recent SK results (14) covering $E_{recoil} \geq 5$ MeV, the observed shape of ϕ_ν is consistent with an undistorted ${}^8\text{B}$ neutrino spectrum shape; a χ^2 fit of the overall spectrum shape resulted in $\chi^2/\text{d.o.f.} = 19.1/18$, without any *Hep* neutrino admixture. This is not too surprising since $\phi_\nu(hep)$ is typically three orders of magnitude smaller than $\phi_\nu({}^8\text{B})$. Meanwhile, by assuming that 1.3 ± 2.0 events registered in the recoil electron energy bin, $E_{recoil} = 18 - 21$ MeV, are due to the *Hep* neutrinos, the 90% confidence level upper limit of $\phi_\nu(hep)$ was determined to be $40 \times 10^3 \text{cm}^{-2} \text{s}^{-1}$ (14). This upper limit is 4.3 times the BP2000 prediction for the no neutrino-oscillation assumption; thus the experimental $\phi_\nu(hep)$ is consistent with the theoretical value. However, BP00 stressed that the significance of this agreement is limited since one cannot assign an estimate of uncertainty to the theoretical value of S_{Hep} used in BP00.

This last point can be greatly improved with the use of the EFT* calculation of S_{Hep} by Park et al. (66, 67), since this calculation gives S_{Hep} with a well-controlled error estimate (in the sense explained earlier). The use of the central value of obtained in (67) would slightly lower $\phi_\nu(hep)^{SSM}$ but with its upper end compatible with $\phi_\nu(hep)^{SSM}$ in (3). Thus, the statement that the upper limit of the experimental $\phi_\nu(hep)$ is ~ 4 times the central value of the SSM prediction remains valid. However, with the use of S_{Hep} obtained in the EFT* calculation, the SSM prediction is now controlled within $\sim 15\%$ precision, and this fact is

expected to be valuable in future analyses of experiments concerning the *Hep* neutrinos.

6 RELATED TOPICS

We have so far concentrated on the calculations of *Hep*. To further clarify the key aspects involved in these calculations, it is informative to discuss the related problems of evaluating the cross sections for the *pp* fusion reaction ($p + p \rightarrow d + e^+ + \nu_e$), the neutrino-deuteron reactions, and the *Hen* reaction.

6.1 The *pp* Fusion Process

The most updated SNPA estimation of the *pp* fusion rate was carried out by Schiavilla et al. (71), using the EXC operator whose strength was normalized to fit $\Gamma_\beta^{\text{tritium}}$. An EFT* calculation of the *pp* fusion rate was done by Park et al. (67, 72), with the use of exactly the same method as employed for the *Hep* calculation. The result is $S_{pp} = 3.94 \times (1 \pm 0.005) \times 10^{-25}$ MeV – b. This EFT* result supports the value of S_{pp} obtained in SNPA (71). It has been found that S_{pp} in the EFT* calculation varies only by $\sim 0.1\%$ against changes in Λ , and this feature can be regarded as typical for unsuppressed transitions such as *pp* fusion. Thus, to the extent that the Λ dependence serves as a reasonable measure of theoretical uncertainties (as discussed earlier), the EFT* prediction of S_{pp} can be considered highly robust. The 0.5% error in the above S_{pp} is dominated by the uncertainty in the experimental value of $\Gamma_\beta^{\text{tritium}}$.

The PDS scheme also was used to estimate the *pp* fusion rate (73). Taking advantage of the fact that the energy and momentum involved in this reaction are very low, “nucleon-only” EFT (without pions) was employed. To the order

considered in (73), there appears one unknown LEC, denoted by L_{1A} , and there have been attempts to constrain the value of L_{1A} using observables in the 2-nucleon systems (74).

6.2 Neutrino-deuteron reactions

The ν - d cross sections for $E_\nu \lesssim 20$ MeV is very important in connection to the SNO experiments. Within SNPA a detailed calculation of the ν - d cross sections, $\sigma(\nu d)$, was carried out by Nakamura et al. (75,76), while Butler, Chen and Kong (BCK) (77) carried out an EFT calculation of $\sigma(\nu d)$, using the PDS scheme (55). The EFT results (77) agree with the SNPA results (76), if the above-mentioned unknown LEC, L_{1A} , involved in the PDS scheme is suitably adjusted. The optimal value, $L_{1A} = 5.6 \text{ fm}^3$, found in (77) is consistent with the order of magnitude of L_{1A} expected from the naturalness argument (based on a dimensional analysis), $|L_{1A}| \leq 6 \text{ fm}^3$. Even though it is reassuring that $\sigma(\nu d)$ calculated in SNPA and EFT agree with each other (in the above-explained sense), it is desirable to carry out an EFT calculation that is free from any adjustable LEC. EFT* allows us to carry out an EFT-controlled parameter-free calculation of $\sigma(\nu d)$, and such a calculation was carried out by Ando et al. (78). The $\sigma(\nu d)$'s obtained in (78) are found to agree within 1% with $\sigma(\nu d)$'s obtained in SNPA (76).

6.3 Hen process

In order to gauge the validity of a calculational method used for *Hep*, it is extremely useful to study as a test case the *Hen* process, ${}^3\text{He} + n \rightarrow {}^4\text{He} + \gamma$, since *Hep* and *Hen* involve similar kinematics and they share the characteristic that

the contribution of the normally dominant 1-body transition operator is highly suppressed due to the symmetry properties of the wave functions. An EFT* calculation of Hen has been carried out by Song and Park (79), and the calculated cross section, $\sigma = (60.1 \pm 3.2 \pm 1.0) \mu\text{b}$, is in reasonable agreement with the experimental values, $(54 \pm 6) \mu\text{b}$ (40), and $(55 \pm 3) \mu\text{b}$ (41). This agreement renders support for the validity of the EFT* approach in general and for the EFT* calculation of Hep in particular, even though there is room for improvements in the p - ^3He continuum wave function used in (79). For the earlier Hen calculations based on SNPA, see (43,80). It is hoped that there will be further investigations of Hen in both SNPA and EFT*.

7 SUMMARY AND OUTLOOKS

As exemplified above, low-energy electroweak processes in light nuclei play important roles in astrophysics, and a recently developed EFT-based formalism, called EFT* or MEEFT (more effective EFT), can be used profitably to calculate the cross sections of these processes with high precision. We have discussed here Hep and a few closely related reactions, but this new method is expected to find uses for other low-energy electroweak processes as well. The numerical results obtained in EFT* generally support those obtained in the conventional SNPA, if the strength of the 2-body current is controlled by the empirical value of an appropriate observable. It is to be stressed that EFT* allows us to make systematic error estimation of the calculated cross sections, a feature that is not readily obtainable in SNPA.

From a formal point of view, one could hope to improve EFT* by employing nuclear wave functions determined in an EFT formalism itself instead of phe-

nomenological wave functions obtained in SNPA. As far as observables that do not involve external currents are concerned, there has been great progress in building a formally consistent EFT approach applicable to complex nuclei (58,81). It will be highly informative to apply this type of formalism to electroweak processes and compare the results with those of EFT*.

Acknowledgment

The authors gratefully acknowledge useful communications with: J.N. Bahcall, M. Rho, M. Fukugita, R. Schiavilla, Y. Suzuki, F. Myhrer, T. Sato, V. Gudkov, D.-P. Min, S. Ando, S. Nakamura and Y.-H. Song. KK's work is supported in part by the NSF, Grant No. PHY-0140214.

Literature Cited

1. Bahcall JN, Ulrich RK. *Rev. Mod. Phys.* 60:297 (1988)
2. Bahcall JN. *Neutrino Astrophysics*. Cambridge: Cambridge University Press (1989)
3. Bahcall JN, Pinsonneault MH, Basu S. *Astrophys. J.* 555:990 (2001)
4. Turck-Chièze S, Lopes I. *Astrophys. J.* 408:347 (1993)
5. Bahcall JN, Peña-Garay C. *JHEP* 0311:004 (2003)
6. Davis R, Harmer DS, Hoffman KC. *Phys. Rev. Lett.* 20:1205 (1968); Rowley JK, Cleveland BT, Davis R. *Solar Neutrinos and Neutrino Astronomy*, eds. ML Cherry, WA Fowler, K Lande. AIP Conference Proceedings No. 126, p. 1. New York: American Institute of Physics (1985)
7. Bahcall JN. *Phys. Rev. Lett.* 12:300 (1964)
8. Fukuda Y, et al. (Kamiokande Collab.) *Phys. Rev. Lett.* 77:1683 (1996)
9. Fukuda Y, et al. (Super-Kamiokande Collab.) *Phys. Rev. Lett.* 81:1158 (1998)
10. Abdurashitov JN, et al. (SAGE Collab.) *Phys. Rev. Lett.* 77:4708 (1996)
11. Anselmann P, et al. (GALLEX Collab.) *Phys. Lett. B* 342:440 (1995); Hampel W, et al. (GALLEX Collab.) *Phys. Lett. B* 388:364 (1996)

12. Ahmad QR, et al. (SNO Collab.) *Phys. Rev. Lett.* 87:071301 (2001)
13. Cleveland BT, et al. *Astrophys. J.* 496:505 (1998)
14. Fukuda S, et al. (Super-Kamiokande Collab.) *Phys. Rev. Lett.* 86:5651 (2001)
15. Gavrin V, et al. Talk at VIII Int'l Conf. on Topics in Astroparticle and Underground Physics (TAUP03), Seattle, Sept. 2003; Abdurashitov JN, et al. *JETP* 95:181 (2002)
16. Hampel W, et al. (GALLEX Collab.) *Phys. Lett. B* 447:127 (1999)
17. Bellotti E. Talk at VIII Int'l Conf. on Topics in Astroparticle and Underground Physics (TAUP03), Seattle, Sept. 2003; Altmann M, et al. (GNO Collab.) *Phys. Lett. B* 490:16 (2000)
18. Ahmad QR, et al. (SNO Collab.) *Phys. Rev. Lett.* 89:011301 (2002)
19. Ahmad QR, et al. (SNO Collab.) *Phys. Rev. Lett.* 89:011302 (2002)
20. Ahmed SN, et al. (SNO Collab.) nucl-ex/0309004
21. Bahcall JN. *Phys. Rep.* 333:47 (2000)
22. Pontecorvo B. *Zh. Eksp. Teor. Fiz.* 33:549 (1957) [*Sov. Phys. JETP* 6:429 (1958)]; *Zh. Eksp. Teor. Fiz.* 34:247 (1958) [*Sov. Phys. JETP* 7:172 (1958)]; *Zh. Eksp. Teor. Fiz.* 53:1717 (1967) [*Sov. Phys. JETP* 26:984 (1968)]; Pontecorvo B. *Phys. Lett. B* 26:630 (1968); Gribov V, Pontecorvo B. *Phys. Lett. B* 28:493 (1969)
23. Maki Z, Nakagawa M, Sakata S. *Prog. Theor. Phys.* 28:870 (1962)
24. Mikheyev SP, Smirnov AYu. *Yad. Fiz.* 42:1441 (1985) [*Sov. J. Nucl. Phys.* 42:913 (1985)]; Wolfenstein L. *Phys. Rev. D* 17:2369 (1978)
25. Fukuda Y, et al. (Super-Kamiokande Collab.) *Phys. Rev. Lett.* 81:1562 (1998)
26. Eguchi K, et al. (KamLAND Collab.) *Phys. Rev. Lett.* 90:021802 (2203)
27. Fukugita M, Yanagida T. *Physics of Neutrinos and Applications to Astrophysics*. Berlin: Springer (2003)
28. Bahcall JN. *Phys. Rev. D* 44:1644 (1991)
29. Fukuda Y, et al. (Super-Kamiokande Collab.) *Phys. Rev. Lett.* 82:2430 (1999)
30. Fukuda S, et al. (Super-Kamiokande Collab.) *Phys. Lett. B* 539:179 (2002)
31. Kuzmin VA. *Phys. Lett.* 17:27 (1965)
32. Escribano R, Frère J-M, Gevaert A, Monderen D. *Phys. Lett. B* 444:397 (1998)
33. Bahcall JN, Krastev PI. *Phys. Lett. B* 436:243 (1998)

34. Marcucci LE, Sciarilla R, Viviani M, Kievsky A, Rosati S, Beacom JF. *Phys. Rev. C* 63:015801 (2001)
35. Salpeter EE. *Phys. Rev.* 88:547 (1952)
36. Werntz C, Brennan JG. *Phys. Rev.* 157:759 (1967)
37. Werntz C, Brennan JG. *Phys. Rev. C* 8:1545 (1973)
38. Tégner PE, Bargholz Chr. *Astrophys. J.* 272:311 (1983)
39. Chemtob M, Rho M. *Nucl. Phys. A* 163:1 (1971)
40. Wolfs FLH, Freedman SJ, Nelson JE, Dewey MS, Greene GL. *Phys. Rev. Lett.* 63:2721 (1989)
41. Wervelman R, Abrahams K, Postma H, Booten JGL, Van Hees AGM. *Nucl. Phys. A* 526:265 (1991)
42. Carlson J, Riska DO, Schiavilla R, Wiringa RB. *Phys. Rev. C* 44:619 (1991)
43. Schiavilla R, Wiringa RB, Pandharipande VR, Carlson J. *Phys. Rev. C* 45:2628 (1992)
44. Horowitz CJ. *Phys. Rev. C* 60:022801 (1999)
45. For a recent review, see, for example, Carlson J, Schiavilla R. *Rev. Mod. Phys.* 70:743 (1998)
46. Riska DO, Brown GE. *Phys. Lett. B* 38:193 (1972); Riska DO. *Phys. Rep.* 181:207 (1989)
47. Ivanov E, Truhlik E. *Nucl. Phys. A* 316:437 (1979); 316:451 (1979); Towner IS. *Phys. Rep.* 155:263 (1987)
48. Weinberg S. *Phys. Lett. B* 251:288 (1990); *Nucl. Phys. B* 363:3 (1991); *Phys. Lett. B* 295:114 (1992)
49. Bernard V, Kaiser N, Meißner U-G. *Int. J. Mod. Phys. E* 4:193 (1995)
50. Brown GE, Rho M. *Phys. Rep.* 363:85 (2002)
51. Georgi H. *Weak Interactions and Modern Particle Physics*. New York: Benjamin (1984)
52. Weinberg S. *Physica* 96A:327 (1979)
53. Gasser J, Leutwyler H, *Ann. Phys.* 158:142 (1984); Gasser J, Sainio M, Švarc A. *Nucl. Phys. B* 307:779 (1988)
54. Jenkins E, Manohar AV. *Phys. Lett. B* 255:558 (1991)
55. Kaplan DB, Savage MJ, Wise MB. *Nucl. Phys. B* 478:629 (1996); *Phys. Lett. B* 424:390 (1998); *Nucl. Phys. B* 534:329 (1998)
56. Beane SR, Bedaque PF, Haxton WC, Phillips DR, Savage MJ. In *At the Frontier of Particle*

- Physics – Handbook of QCD*, ed. M Shifman, 1:133. Singapore: World Scientific (2001)
57. van Kolck U. *Prog. Part. Nucl. Phys.* 43:337 (1999)
58. Bedaque PF, Rupak G, Grißhammer HW, Hammer H-W. *Nucl. Phys. A* 714:589 (2003)
59. Bedaque PF, van Kolck U. *Annu. Rev. Nucl. Part. Sci.* 52:339 (2002)
60. Park T-S, Min D-P, Rho M. *Phys. Rev. Lett.* 74:4153 (1995); *Nucl. Phys. A* 596:515 (1996)
61. Park T-S, Kubodera K, Min D-P, Rho M. *Phys. Rev. C* 58:637 (1998); *Nucl. Phys. A* 646:83 (1999); *Phys. Lett. B* 472:232 (2000); *Nucl. Phys. A (Proc. Suppl.)* 684:101 (2001)
62. Park T-S, Kubodera K, Min D-P, Rho M. *Astrophys. J.* 507:443 (1998)
63. Marcucci LE, Schiavilla R, Viviani M, Kievsky A, Rosati S. *Phys. Rev. Lett.* 84:5959 (2000)
64. Viviani M, Kievsky A, Rosati S. *Few-Body Syst.* 18:25 (1995); Viviani M, Rosati A, Kievsky A. *Phys. Rev. Lett.* 81:1580 (1998)
65. Simpson JJ. *Phys. Rev. C* 35:752 (1987)
66. Park T-S, Marcucci LE, Schiavilla R, Viviani M, Kievsky A, Rosati S, Kubodera K, Min D-P, Rho M. nucl-th/0107012
67. Park T-S, Marcucci LE, Schiavilla R, Viviani M, Kievsky A, Rosati S, Kubodera K, Min D-P, Rho M. *Phys. Rev. C* 67:055206 (2003)
68. Phillips DR, Cohen TD. *Nucl. Phys. A* 668:45 (2000)
69. Bogner S, Kuo TTS, Corragio L. *Nucl. Phys. A (Proc. Suppl.)* 684:432 (2001); Bogner S, Kuo TTS, Corragio L, Covello A, Itaco N. *Phys. Rev. C* 65:051301 (2002)
70. Adelberger EG, et al. *Rev. Mod. Phys.* 70:1265 (1998)
71. Schiavilla R, et al. *Phys. Rev. C* 58:1263 (1998)
72. Park T-S, Marcucci LE, Schiavilla R, Viviani M, Kievsky A, Rosati S, Kubodera K, Min D-P, Rho M. nucl-th/0106025
73. Kong X, Ravendal F. *Nucl. Phys. A* 656:421 (1999); *Nucl. Phys. A* 665:137 (2000); *Phys. Lett. B* 470:1 (1999); Butler M, Chen J-W. *Phys. Lett. B* 520:87 (2001)
74. Butler M, Chen J-W, Vogel P. *Phys. Lett. B* 549:26 (2002); Brown KIT, Butler MN, Guenther DB. nucl-th/0207008; Balantekin AB, Yüksel H. *J. Phys. G:Nucl. Part. Phys.* 29:665 (2003)
75. Nakamura S, Sato T, Gudkov V, Kubodera K. *Phys. Rev. C* 63:034617 (2001)
76. Nakamura S, Sato T, Ando S, Park T-S, Myhrer F, Gudkov V, Kubodera K. *Nucl. Phys.*

- A* 707:561 (2002); *Nucl. Phys. A (Proc. Suppl.)* 721:549 (2003)
77. Butler M, Chen J-W. *Nucl. Phys. A* 675:575 (2000); Butler M, Chen J-W, Kong X. *Phys. Rev. C* 63:035501 (2001)
78. Ando S, Song YH, Park T-S, Fearing HW, Kubodera K. *Phys. Lett. B* 555:49 (2003)
79. Song Y-H, Park T-S. nucl-th/0311055
80. Carlson J, Riska DO, Schiavilla R, Wiringa RB. *Phys. Rev. C* 42:830 (1990)
81. Epelbaum E, Glöckle W, Krüger A, Meißner U-G. *Nucl. Phys. A* 645:413 (1999); Epelbaum E, Glöckle W, Meißner U-G. *Nucl. Phys. A* 671:295 (2000); Epelbaum E, Kamada H, Nogga A, Witala H, Glöckle W, Meißner U-G. *Phys. Rev. Lett.* 86:4787 (2001); Epelbaum E, Nogga A, Glöckle W, Kamada H, Meißner U-G, Witala H. *Phys. Rev. C* 66:064001 (2002); *Eur. Phys. J. A* 15:543 (2002)

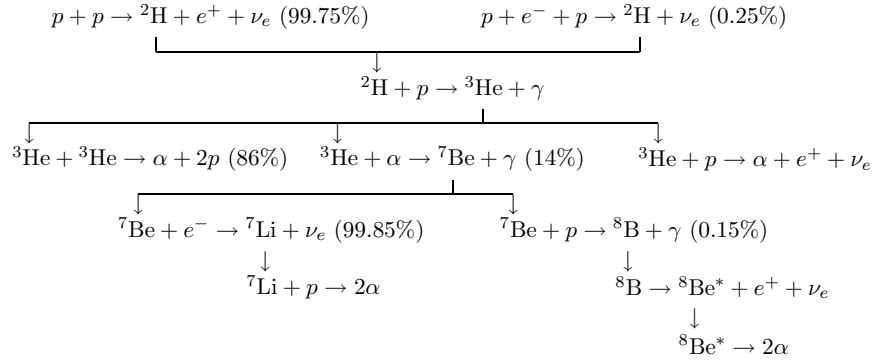


Figure 1: Solar thermonuclear reactions in the pp -chain and their branching ratios. The Hep branching ratio is of the order of 0.01% or less.

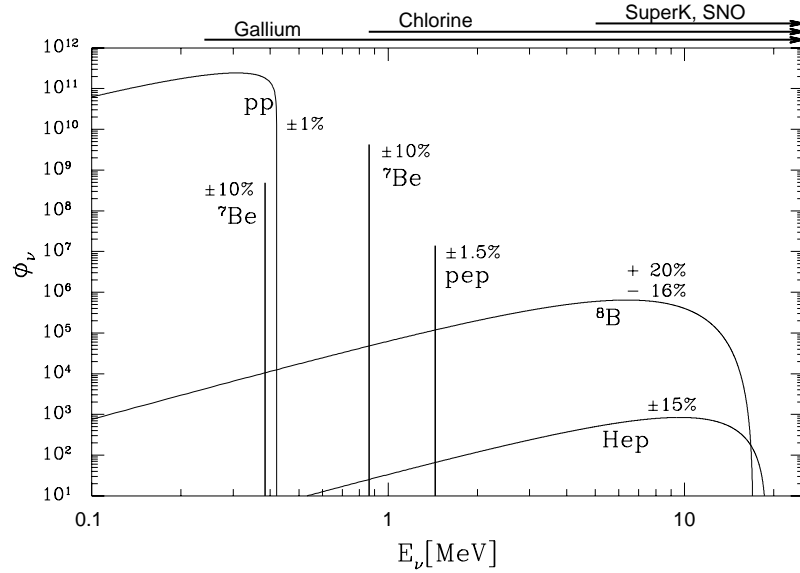


Figure 2: Solar neutrino spectrum ϕ_ν vs the neutrino energy E_ν . The neutrino fluxes from continuum sources are given in units of $\text{cm}^{-2}\text{s}^{-1}\text{MeV}^{-1}$, and the line fluxes in units of $\text{cm}^{-2}\text{s}^{-1}$. The arrows at the top indicate the ranges of E_ν covered by the experiments mentioned in the text.